Supplementary file

Mechanisms of feldspar dissolution and associated authigenic mineral precipitation in coal measure tight sandstone reservoirs: Insights using a reaction-transport numerical model incorporating organic chelation

Weikai Huang[1], Kelai Xi[1,*], Yingchang Cao[1], Xiang Shan[2], Zhicheng Cui[1], and Helge Hellevang[3]

[1] *State Key Laboratory of Deep Oil and Gas, China University of Petroleum (East China), Qingdao 266580, P. R. China*

[2] *PetroChina Hangzhou Institute of Petroleum Geology, Hangzhou 310023, P. R. China*

[3] *Department of Geosciences, University of Oslo, Oslo 0316, Norway*

E-mail address: m15060578935@163.com (W. Huang); xikelai@upc.edu.cn (K. Xi); caoych@upc.edu.cn (Y. Cao); shanx_hz@petrochina.com.cn (X. Shan); Czc@s.upc.edu.cn (Z. Cui); helge.hellevang@geo.uio.no (H. Hellevang)

* Corresponding author (ORCID: 0000-0001-5138-6466 (K. Xi))

Huang, W., Xi, K., Cao, Y., Shan, X., Cui, Z., Hellevang, H. Mechanisms of feldspar dissolution and associated authigenic mineral precipitation in coal measure tight sandstone reservoirs: Insights using a reaction-transport numerical model incorporating organic chelation. Advances in Geo-Energy Research, 2025, 18(1): 51-68.

The link to this file is: https://doi.org/10.46690/ager.2025.10.05

1. Supplementary tables

Table S1. The parameters for the transport module at different temperatures and flow rates.

Temperature (°C)	Flow rate (m/yr)	Total simulation duration (yr)	Cell length (m)	Time step (yr)	Shift
25	10	2,500	0.1	0.01	250,000
25	1	2,500	0.1	0.1	25,000
25	0.1	2,500	0.1	1	2,500
65	1	2,500	0.1	0.1	25,000
65	0.1	2,500	0.1	1	2,500
65	0.01	2,500	0.1	10	250
100	0.1	2,500	0.1	1	2,500
100	0.01	2,500	0.1	10	250
100	0.001	2,500	0.1	100	25
130	0.1	2,500	0.1	1	2,500
130	0.01	2,500	0.1	10	250
130	0.001	2,500	0.1	100	25

Table S2. Standard state dissociation constants for organic chelates with Fe^{2+}, Al^{3+}, Ca^{2+}, Na^{+} and Mg^{2+} used in simulations.

Chelate dissociation reaction	**Log K_{eq}, 25 °C**
$HOxalate^{-} = HOxalate^{-}$	0
$H^{+} + HOxalate^{-} = H_2Oxalate$	4.266
$HOxalate^{-} = Oxalate^{2-} + H+$	-1.252
$Oxalate^{2-} + 2Ca^{2+} = Ca_2Oxalate^{2+}$	3.44
$Oxalate^{2-} + Al^{3+} = AlOxalate^{+}$	7.73
$2Oxalate^{2-} + Al^{3+} = Al(Oxalate)_2^{-}$	12.5
$3Oxalate^{2-} + Al^{3+} = Al(Oxalate)_3^{3-}$	16.4
$Al^{3+} + H^{+} + Oxalate^{2-} = AlHOxalate^{2+}$	7.46
$Al^{3+} + 2Oxalate^{2-} + H_2O = Al(OH)(Oxalate)_2^{2-} + H^{+}$	6.84
$Al^{3+} + Oxalate^{2-} + 2H_2O = Al(OH)_2^{-}(Oxalate)^{-} + H^{+}$	-3.12
$Na^{+} + Oxalate^{2-} = Na(Oxalate)^{-}$	-1.2
$Mg^{+2} + Oxalate^{2-} = Mg(Oxalate)$	2.9
$Fe^{3+} + Oxalate^{2-} = Fe(Oxalate)^{+}$	8.9
$Fe^{3+} + 2\ Oxalate^{2-} = Fe(Oxalate)_2^{-}$	15.7
$Fe^{3+} + 3\ Oxalate^{2-} = Fe(Oxalate)_3^{3-}$	20.4

Table S3. kinetic parameters used in Kinetic module.

Mineral	k_{25} (mol/cm^2/s)	E_a (kJ/mol)	Surface area (cm^2/g)	pH dependence of rate (n)
K-feldspar	8.70×10^{-15}	51.70	9.8	0.5
Albite	6.92×10^{-15}	65.00	9.8	0.457
Anorthite	4.78×10^{-11}	16.60	9.8	1.411
Quartz	1.02×10^{-18}	87.70	9.8	0
Kaolinite	4.9×10^{-16}	65.90	25,000	0.777
Muscovite	1.66×10^{-17}	22.00	325,000	0.37

Table S4. Mineral composition of tight sandstone in Badaowan Formation reservoir.

Well	Depth (m)	Quartz (m)	K-feldspar (m)	Plagioclase (m)	Clay minerals (m)	Calcite (m)	Ferroan calcite (m)	Ankerite (m)
M28	5,128.9	65.77	7.94	23.81	2.48	/	/	/
M28	5,130.79	63.36	9.22	24.19	3.23	/	/	/
M28	5,132.45	62.53	9.09	25.01	3.37	/	/	/
M28	5,134.18	58.06	6.83	23.91	4.37	6.83	/	/
M28	5,135.41	63.94	8.98	24.68	2.40	/	/	/
M28	5,186.22	80.61	4.41	12.15	2.83	/	/	/
M28	5,186.78	75.17	6.73	15.71	2.39	/	/	/
M28	5,188.6	66.20	8.28	21.28	4.24	/	/	/
M28	5,190.09	70.56	7.84	19.04	2.56	/	/	/
M28	5,192.84	75.75	6.49	15.15	2.61	/	/	/
Qs10	4,243.99	52.17	8.70	18.48	1.09	17.39	/	2.17
Qs10	4,247.02	68.58	9.64	20.36	1.42	/	/	/
Qs10	4,654.68	69.41	4.63	20.82	2.83	2.31	/	/
Qs10	4,655.23	67.96	5.66	21.52	2.59	2.27	/	/
Qs10	4,241.51	69.15	8.78	19.76	2.31	/	/	/
Qs10	4,244.28	68.90	9.69	19.38	2.03	/	/	/
Qs10	4,246.78	70.86	7.63	19.62	1.89	/	/	/
Qs10	4,655.72	61.99	13.53	16.91	1.93	5.64	/	/
Qs10	4,656.69	55.85	9.09	28.57	6.49	/	/	/
Sq1	4,321.06	54.96	12.59	26.33	6.12	/	/	/
Sq1	4,321.95	57.76	12.84	25.67	3.73	/	/	/
Sq1	4,322.99	56.98	11.61	25.33	3.97	/	2.11	/
Sq1	4,324.98	57.55	11.31	26.72	4.42	/	/	/
Sq1	4,326.26	59.60	9.58	25.54	3.15	/	2.13	/
Sq1	4,328.03	55.82	13.13	26.27	4.78	/	/	/
Ft1	5,364	56.90	11.13	28.45	3.52	/	/	/
Ft1	5,714	59.82	9.97	26.17	4.04	/	/	/

Table S5. The amount of feldspar dissolution, quartz overgrowth and authigenic kaolinite on the cast thin section in Badaowan Formation tight sandstone, Junggar Basin.

Well	Depth (m)	Formation	Porosity (m)	Feldspar dissolution (m)	Kaolinite precipitation (m)	Quartz overgrowth (m)
Sq1	4,323.4	J_1b^3	10.4	1.84	1.05	1.18
Sq1	4,325.2	J_1b^3	10.1	1.93	0.84	1.03
Sq1	4,326.35	J_1b^3	9.7	1.92	1.41	1.30
Sq1	4,327.1	J_1b^3	8.1	1.21	0.74	1.16
Sq1	4,330.8	J_1b^3	6.5	0.89	0.32	0.60
Sq1	4,331.6	J_1b^3	8	1.28	0.48	0.81
Sq1	4,332.13	J_1b^3	8.6	1.41	0.44	1.17
Sq1	4,396.4	J_1b^3	6.1	1.48	1.12	1.21
Qs10	4,240.7	J_1b^3	10.3	1.96	1.85	1.22
Qs10	4,241.5	J_1b^3	8.6	1.32	1.88	0.95
Qs10	4,242.23	J_1b^3	9.0	1.23	1.4	1.41
Qs10	4,244.68	J_1b^3	7.3	2.08	1.03	2.03
Qs10	4,245.22	J_1b^3	9.4	1.75	1.06	1.00
Qs10	4,654.57	J_1b^1	6	0.69	0.95	0.69
Qs10	4,655.42	J_1b^1	6.0	0.6	0.72	1.98
M28	4,762.35	J_1b^3	7.7	1.57	0.81	1.33
M28	4,766.7	J_1b^3	8.5	1.58	1.02	0.80
M28	4,767.8	J_1b^3	6.7	0.94	0.46	0.76
M28	4,768.85	J_1b^3	8.9	1.31	1.6	0.56
M28	5,128.45	J_1b^1	11.9	2.57	1.33	1.42
M28	5,129.25	J_1b^1	13	2.93	1.76	1.58
M28	5,132.3	J_1b^1	11.5	2.86	1.58	1.61
M28	5,135.25	J_1b^1	11.8	2.07	1.25	1.18
M28	5,186.1	J_1b^1	11.8	2.1	0.7	1.57
M28	5,186.4	J_1b^1	9.7	1.42	0.68	1.23
M28	5,188.6	J_1b^1	10.7	2	1.08	0.98
M28	5,189.3	J_1b^1	10.2	2.7	1.2	1.35
M28	5,189.8	J_1b^1	10.6	2.2	0.79	1.05
M28	5,191.3	J_1b^1	10.8	1.22	0.75	1.20
M25	4,569.48	J_1b^3	7.0	1.17	1.36	0.42
M25	4,573.75	J_1b^3	7.2	1.09	0.76	2.01
M25	4,574.5	J_1b^3	7.8	1.56	0.63	1.71
M25	5,072.3	J_1b^1	9.9	2.52	1.12	1.54
M25	5,073.8	J_1b^1	12.1	2.31	0.98	1.92

2. Distribution of feldspar dissolution and related authigenic minerals

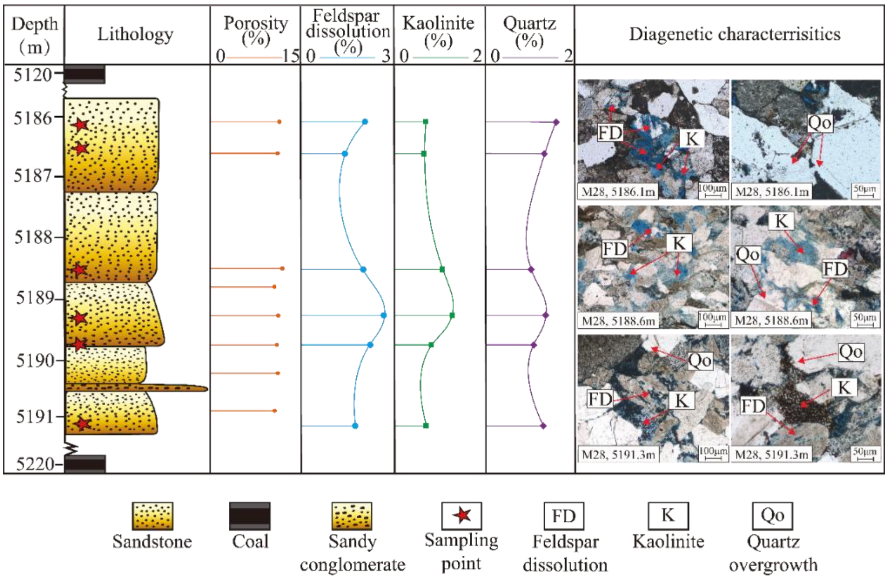

Fig. S1. Distribution characteristics of feldspar dissolution and related authigenic minerals in M28 well.

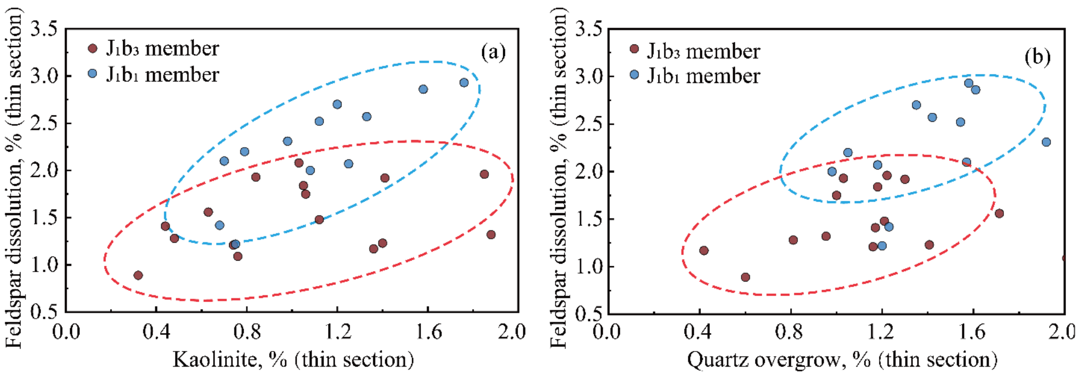

Fig. S2. Relationship between feldspar dissolution, kaolinite and quartz overgrowth. (a) Relationship of feldspar dissolution and kaolinite (thin section) and (b) relationship of feldspar dissolution and quartz overgrowth (thin section).

3. Result of react-transport models at 25 °C and 130 °C

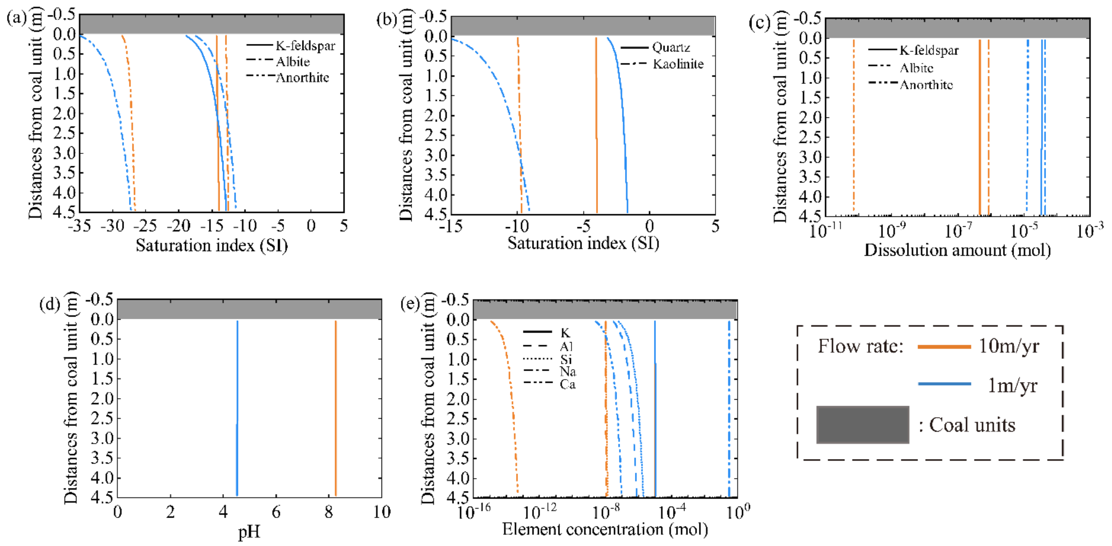

Fig. S3. Model outputs of (a)-(b) mineral saturation index, (c) dissolution amount, (d) pH, and (e) element concentration at 25°C and flow rates of 10 m/yr and 1 m/yr

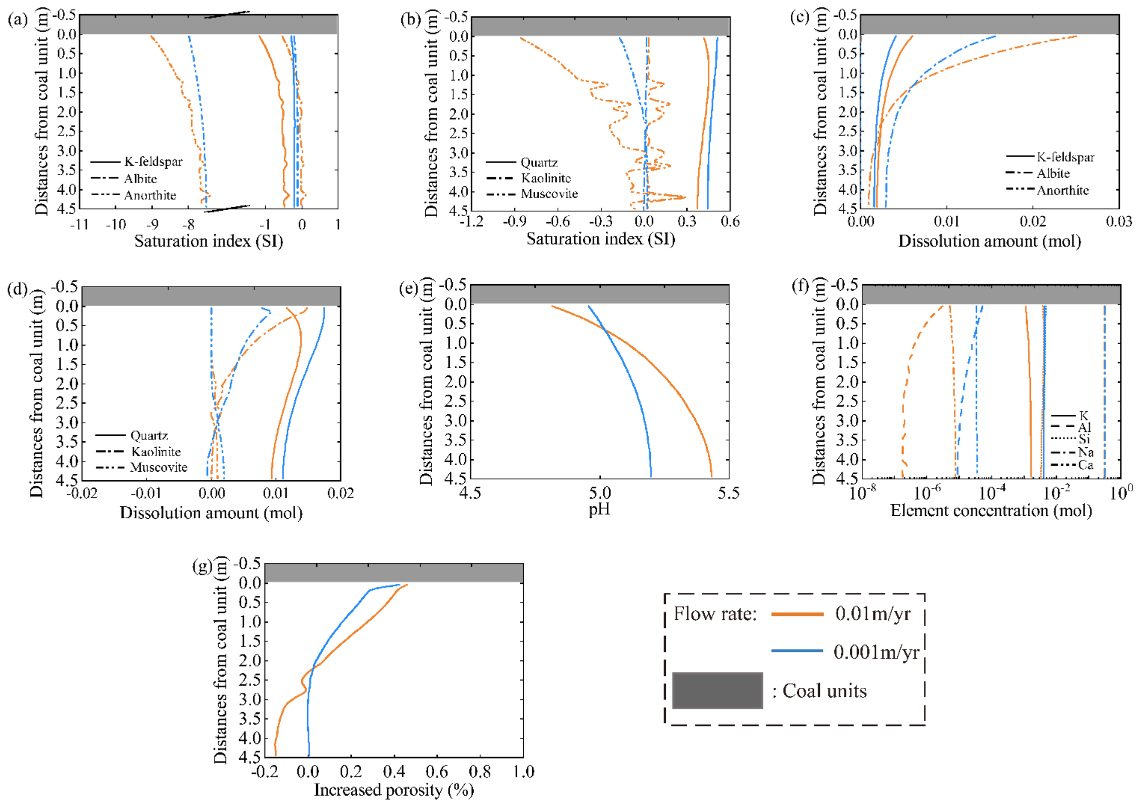

Fig. S4. Model outputs of (a)-(b) mineral saturation index, (c) dissolution amount, (d) precipitation amount, (e) pH, and (f) element concentration (g) increased porosity at 130 °C and flow rates of 0.01 m/yr and 0.001 m/yr.

Evolutionary model of feldspar dissolution and authigenic mineral precipitation in sandstone-coal lithofacies combinations.